Supplementary Materials

Highly Sensitive Detection of Alpha-Fetoprotein Using Sandwich Sensors

Bing Xie[1], Huixing Wang [2], Zaina Omary Mochiwa[2], Dingjie Zhou [3],* and Li Gao [2]*

1 The Fourth Affiliated Hospital of Jiangsu University, Zhenjiang 212001, China;

2 School of Life Sciences, Jiangsu University, Zhenjiang 212013, China;

3 Jiangsu Provincial Health Research Center, Nanjing 210008, China.

Authors to whom correspondence should be addressed.

1. Detection principle and preparation method of AuNPs-Based sensor

A biosensor was designed to detect AFP based on gold nanoparticles and aptamers with AIE molecule (DSAI), an aggregation-induced luminescence effect (Fig.S1). The combination of ammonium cation of DSAI with phosphate anion in aptamer makes the biosensor platform carry stable fluorescence. When gold nanoparticles were added into the system, the aptamers with fluorescence were fixed on the surface of gold nanoparticles due to the strong binding of Au-S. According to the FRET principle, the fluorescence decreased to a certain extent. After adding the AFP, the aptamers were specifically bound to AFP, and the conformation of aptamers was changed. Some aptamers have a tendency towards detachment from the surface of gold nanoparticles, and the fluorescence was restored. The AFP can be detected according to the fluorescence intensity change before and after adding AFP.
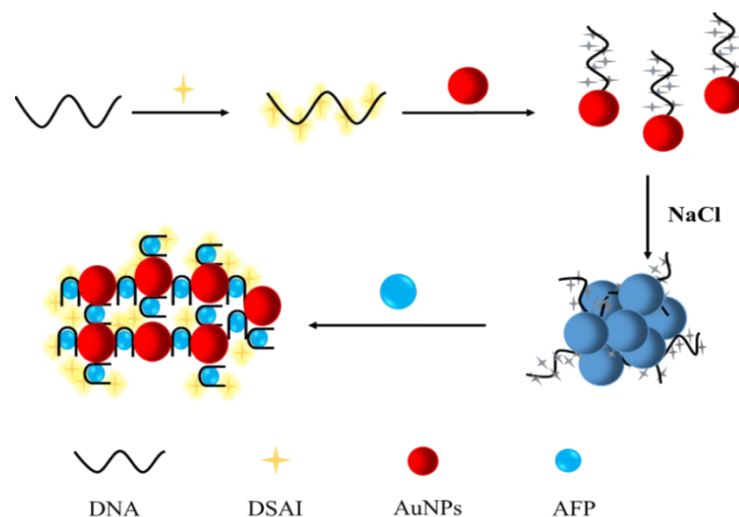
Fig.S1. Schematic diagram of AFP detection by fluorescence sensor based on gold nanoparticles (AuNPs) and aptamer DNA

The final volume was 10 µL. The results indicate that the system contained 10 µM of DSAI and 30 nM of aptamer in a 500 µL volume. After incubation in PBS buffer (100 mM NaCl, pH 7.4) for 15 min, AuNPs with a final concentration of 0.6 nM were added. Following a 12 h reaction period, the mixture was centrifuged at 12,000 rpm for 30 minutes to separate the supernatant from the precipitate. The fluorescence value, F0, was then measured from the supernatant. Subsequently, different concentrations of AFP were added into the system, and the reaction time was 30 min at room temperature to measure its fluorescence value, F. The F / F_0-1 value of the reaction system was obtained by unified data processing with Origin 8.0.

2. Stability of DSAI

To explore the stability of DSAI in solution, a certain concentration of DSAI (10 µM) was used. The change in fluorescence intensity was measured. The results are shown in Fig. S2. It showed that the fluorescence intensity of DSAI remained relatively stable in 30 min. DSAI showed a better stable state under the same concentration and the same buffer system.
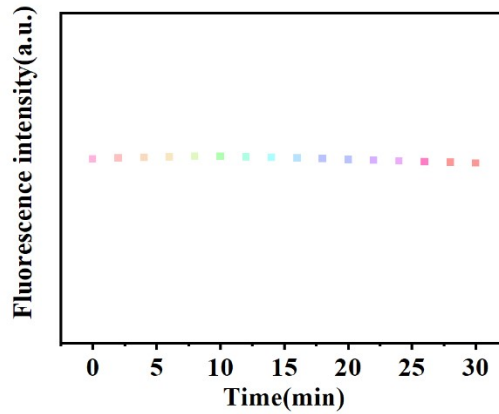
Fig.S2. Fluorescence stabilization kinetics of DSAI molecule in PBS buffer system

3. Optimization of experimental conditions based on gold nanoparticle sensor

In order to achieve the best detection effect of AFP, the experimental conditions were optimized in this study, including the concentration of AuNPs, NaCl, and DNA-SH.

3.1 Optimization of concentration of gold nanoparticles

The concentration of AuNPs was optimized. Different concentrations of AuNPs (0.1 nM, 0.3 nM, 0.6 nM, 0.9 nM, and 1.2 nM) were added into the PBS buffer system; the fluorescence intensity was measured and recorded before and after adding AFP. The change in the recorded fluorescence intensity was compared. The results are shown in Fig.S3. It can be observed from the results in Fig. S3 (a) that with the increasing concentration of AuNP. The fluorescence value of the sensing system was lower and lower due to the combination of AuNPs and aptamer. At the same time, Fig. S3(b) shows that with the increasing concentration of AuNPs, the fluorescence growth rate (F / F_0-1) was also increasing. The F / F_0-1 ratio caused by AuNPs reached the maximum at a concentration of 0.6 nM. With the increase in the concentration of AuNPs, the fluorescence value of the sensing system becomes lower and lower due to the combination of AuNPs and aptamers in Fig. S3 (a). While Fig.S3 (b) showed that the increase in the concentration of AuNPs, the fluorescence growth rate (F/F_0-1) also

increased. The F / F_0-1 ratio induced by AuNPs reached the maximum at 0.6 nM.
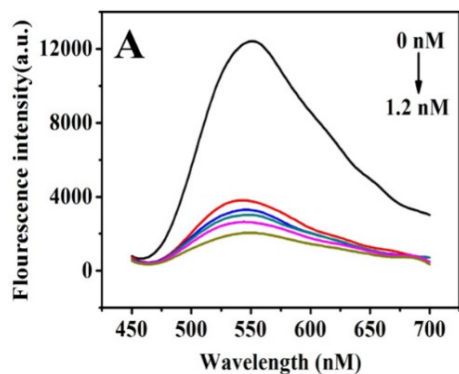

Fig.S3. Fluorescence intensity (A) and Changes in fluorescence intensity (B) induced by AuNPs of different concentrations

3.2 Optimization of sodium chloride concentration

A certain concentration of NaCl can make the gold nanoparticles aggregate and improve the combination of aptamer and Au NPs to a certain extent. Therefore, the influence of different concentrations of NaCl on the fluorescence sensor was further explored in this study. Different concentrations of NaCl (0, 50, 100, 150, and 200 mM) were selected for the optimization experiment. Fig. S4 showed that the F / F_0-1 caused by different concentrations of NaCl was higher than that caused by the absence of NaCl in the system, and the results were consistent with the principle. When the concentration of NaCl was 100 mM, the change in fluorescence intensity was the largest. When the concentration of NaCl continues to increase, it may cause excessive aggregation of AuNPs, which may hinder the binding with the terminal sulfhydryl group of aptamers and reduce the recovery rate of fluorescence intensity in the system. Therefore, 100 mM NaCl was chosen as the best concentration in this experiment.
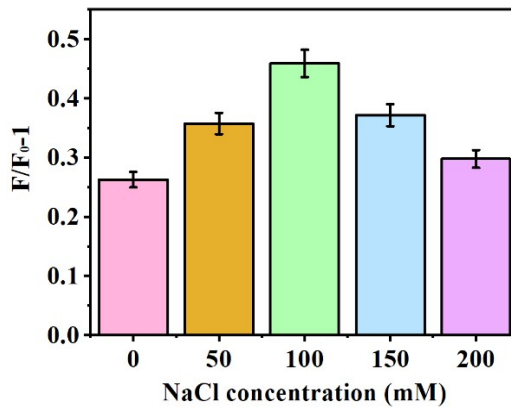
Fig.S4. Effects of different concentrations of NaCl on fluorescence intensity

3.3 Optimization of aptamer concentration

Similarly, different concentrations of aptamers (10, 20, 30, 40, and 50 nM) were optimized in Fig. S5. It can be seen from the figure that the size of the DNA concentration had a significant impact on the sensor. Within a certain range, the size of F / F_0-1 will increase with the increase of aptamer concentration when the concentration of aptamer is 30 nM. F/F_0-1 was the maximum. With the increasing DNA concentration, the change rate of fluorescence intensity decreased gradually. Therefore, 30 nM DNA was chosen as the optimal concentration for this experiment.
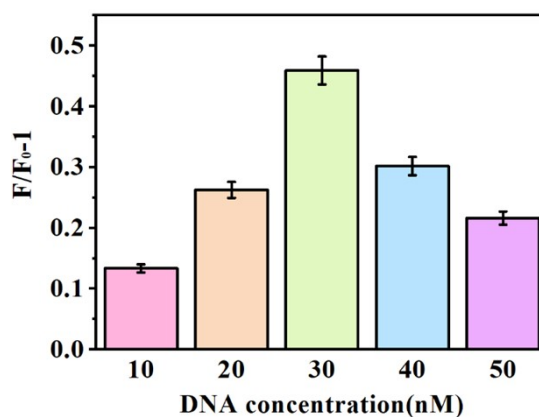

Fig.S5. Influence of aptamer DNA on fluorescence intensity

3.4 Sensitivity test

Different concentrations of AFP (0.01, 0.05, 0.1, 0.5, 0.8, 1, 5, 8, and 10 ng/mL)

were added to the sensing system. The reaction system was mixed evenly and incubated at room temperature for 30 min. The fluorescence intensity was measured and recorded under the excitation of 428 nm and emission of 550 nm. It can be observed from the result in Fig. S6. The fluorescence intensity after adding AFP was increased compared with and without AFP. Specifically, there was an obvious linear relationship between F/F_0-1 and AFP concentration in the range of 0.01-1 ng / mL, and the linear regression equation was $F/F_0-1 = 0.2819 \times C [AFP] + 0.1795$, $R^2=0.99$. With the further increase of AFP concentration, the fluorescence of AFP increased slowly. Based on 3S / N, the detection limit was 4.81 pg / mL.
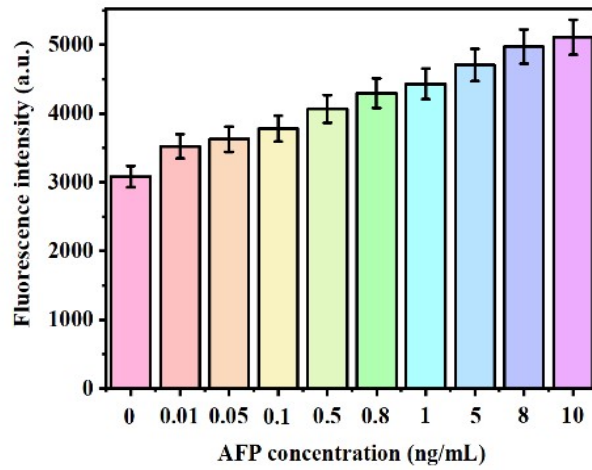
(a)
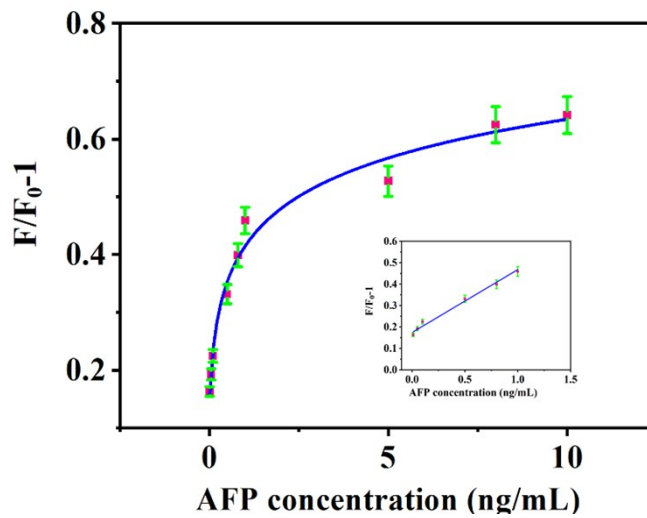
(b)

Fig.S6. Fluorescence intensity (A) and F/F_0-1 (B) changes induced by adding different concentrations of AFP

3.5 Optimization of experimental conditions based on GDYO/AuNPs composite sensor

As a new type of two-dimensional planar carbon nanomaterials, GDYO also showed good properties, such as the structural characteristics of a benzene ring and diyne bond, high electron transfer rate and catalytic properties, and easy surface functionalization. In this experiment, GDYO and AuNPs were synthesized to explore the influence on the biological platform（Fig.S7）.
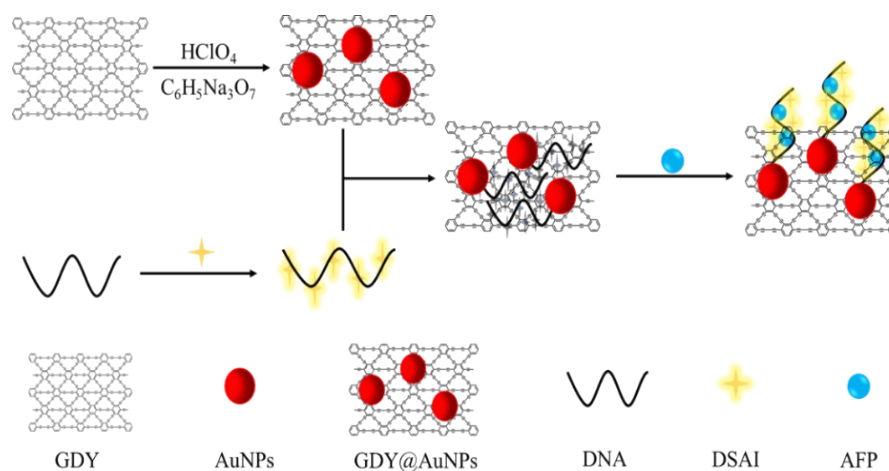

Fig.S7. Schematic diagram of AFP detection principle of fluorescence biosensor based on GDYO@AuNPs and aptamer DNA

4. Preparation of GDYO@AuNPs composite

According to Khalil et al. [30], gold salt was reduced by citric acid. The GDYO@AuNPs composite was made with a few modifications to this method. 20 mL of ultrasonic uniform GDYO (0.5 mg / mL) was added to 100 ml of $HAuCl_4$ (1 mM) and aged for 30 min under the continuous stirring conditions to promote the π-π interaction between Au (III) and the surface of GDYO. The mixture was heated to

80 ℃. 2 mL of sodium citrate solution (300 mM) was added to the system, mixed evenly, and stirred at 80 ℃ for 4 h. The obtained complex was centrifuged (6000 rpm, 2 h) to remove the excess $HAuCl_4$ and other free molecules and then dried in a freeze dryer to obtain GDYO@AuNPs. The composite was dissolved in ultrapure water to prepare a 2 mg/mL solution uniformly dispersed by ultrasound.

4.1 Characterization of AuNPs and GDYO@AuNPs

The Au NPs solution prepared in the laboratory is shown in Fig. S8 (a). The average particle size of AuNPs was about 15 nm, and the standard deviation was 1-2 nm (Fig. S8 (B, C)); it was consistent with the results reported by Li et al. [28]. According to Lambert Beer law, A = εlc (A is the absorbance, ε is the absorption coefficient, about 3.0×10^8, 1 is the path length, about 1 cm, and C is the concentration of the solution).
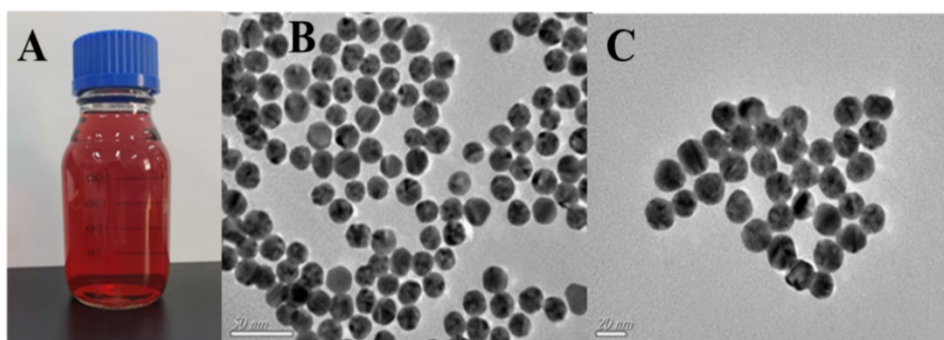

Fig. S8 Preparation solution of gold nanoparticles and transmission electron microscope (TEM)

Suppose the excellent photonic and electronic properties of AuNPs are combined with the excellent structural properties of GDYO. In that case, the overall composite may give better play to the superior properties of nanomaterials. Fig.S9 (a) showed the TEM of GDYO and GDYO@AuNPs. Figure (b) TEM diagram shows that the GDYO was yellow-brown liquid and GDYO@AuNPs. The composite was changed into a black-purple liquid form due to the action of $HAuCl_4$.
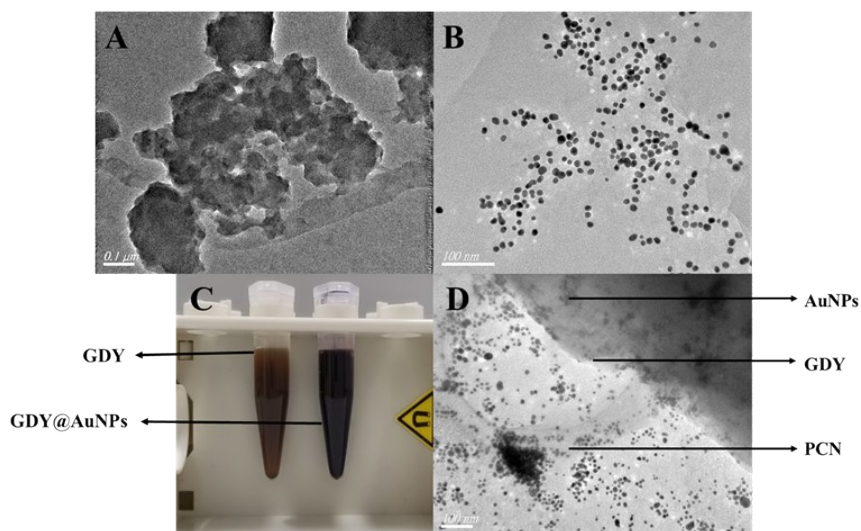
Fig.S9. GDYO and GDYO@AuNPs TEM images (A, B), color contrast (C) and GDYO@AuNPs@PCN TEM images (D).

4.2 Selection of GDYO@AuNPs composite concentration

The effects of different concentrations of GDYO@AuNPs composite (5, 10, 15, 20, and 25 µg/mL) were optimized. The concentration of aptamer is 30 nM. AFP was introduced at a concentration of 0.5 ng/mL. The F / F_0-1 ratio was the highest at the concentration of 15 µg/mL. The F / F_0-1 ratio decreased with the increase in complex concentration. The optimal concentration of the composite was 15 µg/mL.
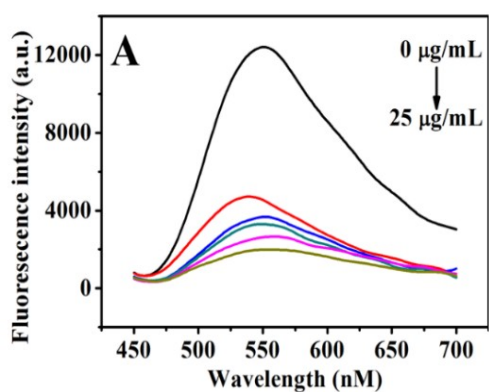

Fig.S10. Fluorescence intensity (A) and changes in fluorescence intensity (B) induced by different concentrations of GDYO@AuNPs composite.

4.3 Selection of aptamer concentration

The influence of different concentrations of aptamers (10, 20, 30, 40, and 50 nM) was explored for the fluorescence intensity. The concentration of the composite was 15 μg/mL. AFP was introduced at a concentration of 0.5 ng/mL. The results are shown in Fig. S11. Compared with Fig. S11, the optimal concentration was 30 nM. This indicated that aptamer concentration had much effect on the whole sensor system. Therefore, 30 nM aptamer was chosen as the optimal concentration in the subsequent experiments.
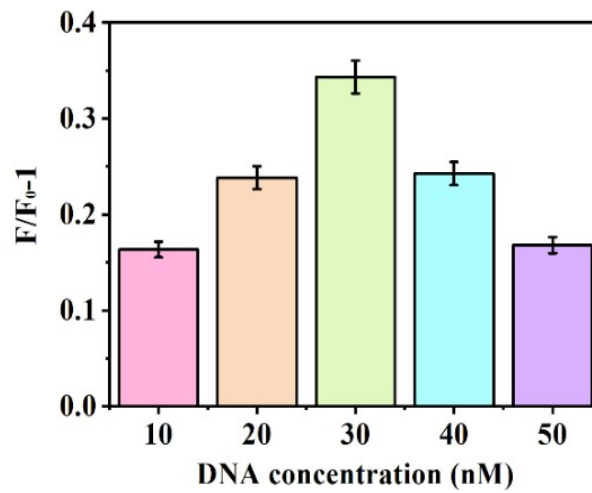

Fig.S11. Influence of aptamer on fluorescence intensity

4.4 Sensitivity analysis of GDYO@AuNPs composite

30 nM aptamer was chosen for the experiments in the PBS buffer system. Different concentrations of AFP (0.01, 0.05, 0.08, 0.1, 0.5, 0.8, 5, and 10 ng / mL) were added to the sensing system. The reaction system was mixed evenly and incubated at room temperature for 30 min. The fluorescence intensity change was measured and recorded at the excitation wavelength of 428 nm. The emission wavelength range was 550 nm. The results are shown in Fig.S12. Specifically, there was an obvious linear relationship between F/F_0-1 and AFP concentration in the range of 0.01-0.1 ng/mL, and the linear regression equation was $F / F_0-1 = 0.6451 \times$

C〔AFP〕+ 0.1627, R^2= 0.98. With the increase in AFP concentration, the fluorescence increased slowly. After adding GDYO, the sensitivity of the biosensor for AFP in this study decreased from 4.81 pg / mL to 3.65 pg / mL based on 3S/N.
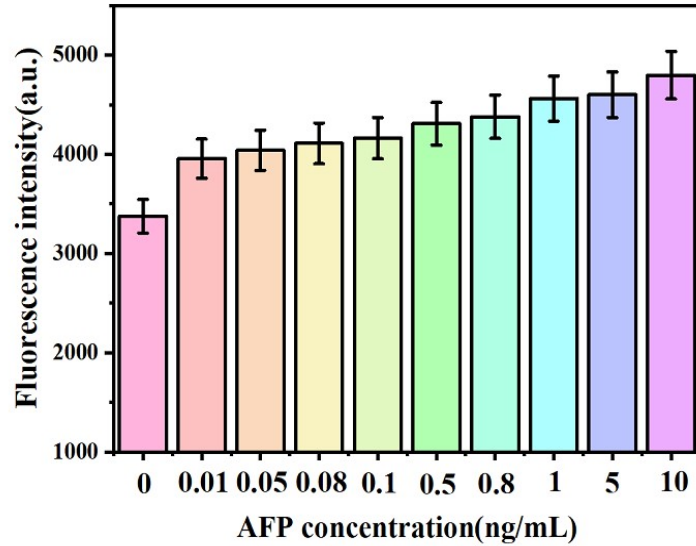

(A)
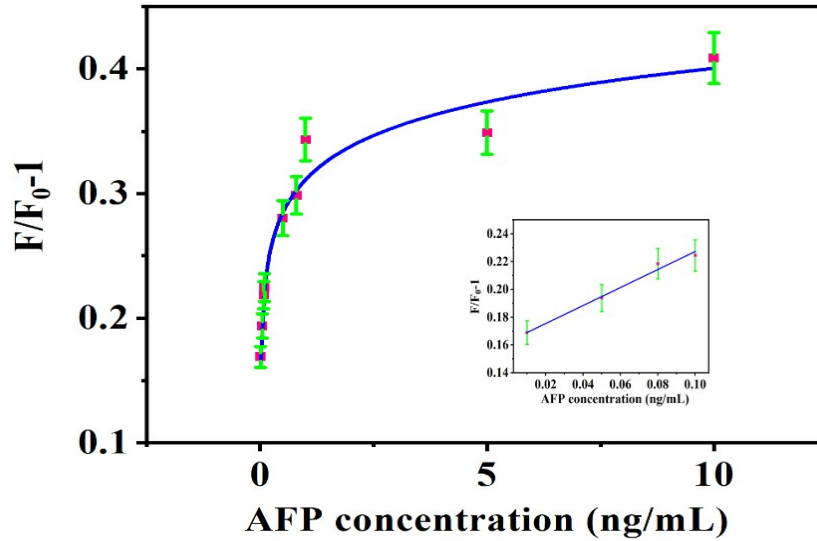
(B)

Fig.S12. Change of fluorescence intensity (A) and F/F_0-1 (B) induced by adding different concentrations of AFP under the condition of 15 μg/mL GDYO@AuNPs

4.5 Sensitivity analysis of GDYO@AuNPs@PCN compound

In this study, sensitivity analysis was conducted utilizing the "three-in-one" nanomaterial. The sensor's performance was compared with that of monocomponent (AuNPs) and bicomponent (GDYO@AuNPs) nanomaterials to understand the rationale behind combining these materials. Different concentrations of AFP (0.005, 0.01, 0.08, 0.1, 0.8, 1, 5, and 10 ng/mL) were introduced to the sensing platform, and the resulting fluorescence spectra were recorded and analyzed using a multi-functional microplate reader (Figure S13a). Furthermore, a clear linear relationship between the recovery value of fluorescence intensity and the concentration of AFP (0.005-0.1 ng/mL) was observed in Figure S13b. The linear regression equation was $F/F_0-1 = 1.773 \times C$ [AFP] + 0.192, with an $R^2 = 0.99$. As the concentration of AFP increased, F/F_0-1 also increased gradually. Based on the signal-to-noise ratio (3S/N), the detection limit of the GDYO@AuNPs@PCN sensor was determined to be 3.39 pg/mL, indicating improved sensitivity. Initially, a sensor for AFP detection was designed using Au NPs functionalized with aptamers under the induction of NaCl (refer to Figures S1, S2, S3, S4, and S5). The detection limit using AuNPs alone was determined to be 4.81 pg/mL (refer to Figure S6). Subsequently, this detection limit was further improved to 3.65 pg/mL using the GDYO@AuNPs sensors (refer to Figures S7, S8, S9, S10, S11, and S12). Additionally, a "three-in-one" composite comprising porous metal crystal material PCN, GDYO, and AuNPs was formed to explore its sensitivity, leveraging the synergistic quenching effect of the three components. Remarkably, the detection limit achieved was 3.39 pg/mL.
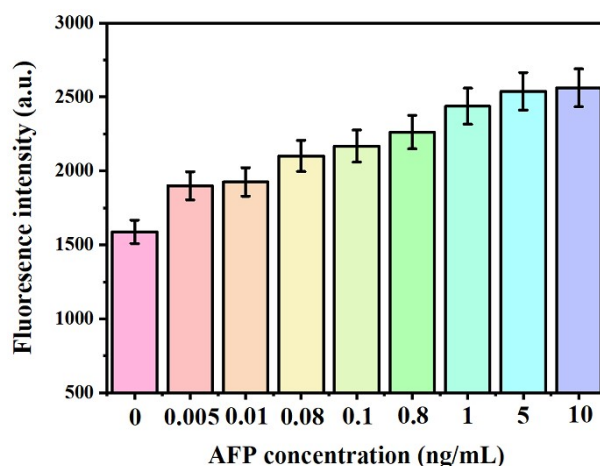
(A)
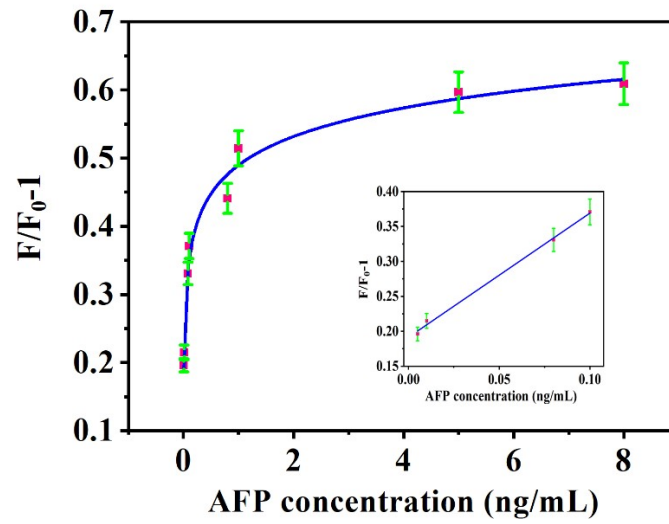
(B)

Fig.S13. (A) Changes in fluorescence intensity and (B) F/F_0-1 were induced by adding different concentrations of AFP.